

# A spatiotemporal analysis of landscape change using an integrated Markov chain and cellular automata models

Hamidreza Keshtkar<sup>1</sup> · Winfried Voigt<sup>1</sup>

Received: 9 December 2015 / Accepted: 10 December 2015 / Published online: 23 December 2015  
© Springer International Publishing Switzerland 2015

**Abstract** Spatially land-cover models are necessary for sustainable land-cover planning. The expansion of human-built land involves the destruction of forests, meadows and farmlands as well as conversion of these areas to urban and industrial areas which will result in significant effects on ecosystems. Monitoring the process of these changes and planning for sustainable use of land can be successfully achieved by using the remote sensing multi-temporal data, spatial criteria and predictor models. In this study, land-cover change analysis and modeling was performed for our study area in central Germany. An integrated Cellular Automata–Markov Chain land change model was carried out to simulate the future landscape change during the period of 2020–2050. The predictive power of the model was successfully evaluated using Kappa indices. As a consequence, land change model predicts very well a continuing downward trend in grassland, farmland and forest areas, as well as a growing tendency in built-up areas. Hence, if the current trends of change continue regardless of the actions of sustainable development, drastic natural area decline will ensue. The results of this study can help local authorities to better understanding the current situation and possible future conditions as well as adopt appropriate strategies for management of land-cover. In this case, they can create a balance between urban development and environmental protection.

**Keywords** Land-cover change · Markov chain · Cellular automata · Multi criteria evaluation

---

✉ Hamidreza Keshtkar  
Hamidreza.keshtkar@uni-jena.de

<sup>1</sup> Institute of Ecology, University of Jena, 07743 Jena, Germany

## Introduction

Many interacting components affect the global environment change and land-cover change is probably one of the most important components which has a significant impact on ecological systems (Vitousek 1994). Land-cover has long been faced with changes and probably will change in the future as well (Ramankutty and Foley 1998). These changes are occurring in different scales (local to global) and in different time periods (days to millennia) (Townshend et al. 1991).

Regional and/or local mapping of land-cover changes is important because it can provide input data for environmental models dealing with topics such as species distributions, climate change and sustainable development policies, or spatial planning and flood risk assessment (Castella 2007; Funkenberg et al. 2014; Kuenzer et al. 2014; Leinenkugel et al. 2013; Pompe et al. 2008).

The unprecedented rate of land change has become a major concern around the world that's why this issue has affected the environmental services and biodiversity at the global level. Both anthropogenic and natural forces are responsible for these changes in Earth's surface. Anthropogenic forces such as urban expansion and the destruction of forests and meadows for economic purposes (development of agricultural land); and natural forces such as fire, flood and tsunamis; have changed the type of land-cover and land-cover all over the world. In recent decades, the changes caused by anthropogenic forces have found a faster pace than natural variations. This is because technological development and population growth are the two main factors which are responsible for the anthropogenic changes and has been unprecedented growth in past two decades. As a result, human has significantly changed almost all the world's ecosystems or is going to change

them; and therefore the capacity of ecosystems to provide goods and services is going to be reduced (Lambin and Meyfroidt 2011).

Due to the rapid and unprec-edented land-cover changes in recent decades, negative consequences such as decline of biodiversity (Balmford et al. 2001; Pimm and Raven 2000; Sala et al. 2000), soil erosion (Sidle et al. 2006), destabilization of watersheds (Rai and Sharma 1998), increasing levels of greenhouse gas emissions (Macedo et al. 2013), water pollution, and air pollution (Houghton 1994) have increased. Also, substantial evidence has been emphasized that land-cover changes significantly influence the geographical distributions of species and the rate of changes in distribution (Jetz et al. 2007; Pompe et al. 2008). Land-cover changes can affect dispersal of plant species directly through changing the quality and quantity of habitat suitability and indirectly via increasing, decreasing, or eliminating dispersal barriers.

Understanding land change trends has been a matter of interest and concern among landscape planners and ecologists (Bagan and Yamagata 2012; Deng et al. 2008). The prediction of land-cover change is a frequently required but difficult process. Effective analysis of land-cover changes require a considerable amount of data about the Earth's surface. Remote sensing prepares a great source of data, from which updated land-cover maps and changes can be analyzed and predicted efficiently. With recent advances in geographic information systems (GIS) and remote sensing tools and modules enable researchers to predict future land-cover changes effectively.

Several statistical and geospatial models have been used to model land-cover change, including logistic regression models (Hu and Lo 2007), neural networks (Basse et al. 2014; Pijanowski et al. 2002), Markov chains (Kamusoko et al. 2009), and cellular automata (CA; Poelmans and Van Rompaey 2010). These approaches are often combined together to create a hybrid model.

In this research, we applied a cellular automata–Markov chain model (CA–Markov) to simulate future land-cover changes. Both CA and the Markov chain model have great advantages in the study on land-cover changes (Sang et al. 2011). Markov-Chain model is one of the most widely used methods for quantifying the probability of land-cover change from state A to state B (e.g. forest to built-up area) in discrete time stages. These probabilities then enter into the CA model to predict spatial changes over a specific time period (Mitsova et al. 2011; Yang et al. 2012). CA–Markov model is based on the initial distribution and transition matrix; it assumes that the drivers, which have created the current situation for the region land-cover, will continue to operate as before in the future (Guan et al. 2011). In many studies, the combination of remote sensing

and GIS are effectively used in CA–Markov model (Mitsova et al. 2011; Subedi et al. 2013).

The objective of this study is to simulate future land-cover changes based on the CA–Markov model in our study area which is located in central Germany. Firstly, transition matrices are computed from the land-cover maps (1990, 2000 and 2010) using the Markov model to forecast area change of land-cover. Secondly, an integration evaluation procedure is used to generate transition suitability maps based on change drivers. Finally, transition matrix and transition suitability map are implemented in the CA–Markov model to simulate spatial distribution of land-cover from 2010 to 2050.

## Materials and methods

### Study areas

The study area is located in central Germany and covers 690000 hectares (Fig. 1). Elevation ranges from 114 to 982 m.a.s.l, with higher elevations concentrated in the Grosser Beerberg Mountain located in the Thuringian Forest. The predominant climate is of the continental type with an average annual rainfall of 604 mm, and an average annual air temperature of 8.6 °C (based on monthly recording data of 18 stations, in the Free state of Thuringia from 1960 to 1990). The soil parent material is mainly calcareous. The landscape maps presented five classes: forest, built-up area, grassland, farmland, and water bodies (lakes, rivers, ponds, and reservoirs).

### Modeling framework

In this section, we describe the main components used for the land-cover changes in future. The process occurs in a raster data environment, most often a grid of uniform cells of a specified resolution. The workflow that was carried out in this study consists of: (1) land-cover mapping of 1990, 2000 and 2010 using the classification of satellite images, (2) computation of transition area matrix derived from a Markov process, indicating the number of pixels to be expected to change each land-cover class to another class over a specified time interval (1990–2000, 2000–2010); (3) getting transition suitability images by Markov chain and multi-criteria evaluation (MCE) model (These suitability images imply the suitability of each cell for a particular land-cover); (4) Evaluating the predictive power of the model by comparing the difference between the actual and projected maps of year 2010; and finally, (5) land-cover change simulation using CA–Markov module for 2020, 2030, 2040, and 2050.

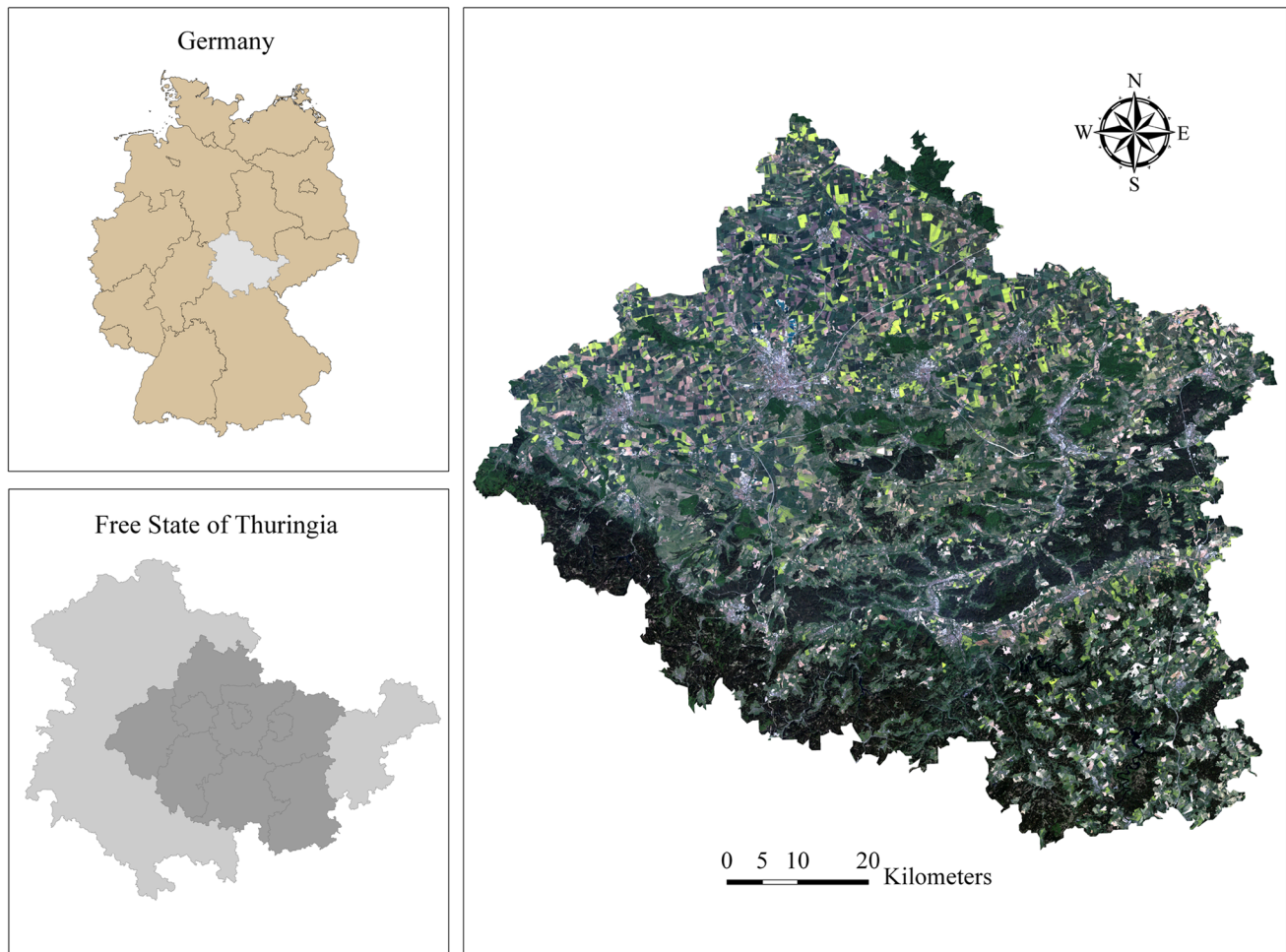


**Fig. 1** Location and land-cover (true color image) of study area for the year 2010

### *Land-cover mapping*

A temporal coverage of Landsat TM and ETM + images (USGS Global Visualization Viewer) from 1990 to 2010 was collected. Using the landsat images in 1990, 2000 and 2010, the land-cover maps were generated for the three corresponding years. To remove the distortions, noises, and errors produced during the imaging process, pre-processing techniques (both geometrically and atmospherically) were applied to all the images. After geometric and atmospheric corrections, the land-cover maps were derived from object-based support vector machine (SVM) classification method (Duro et al. 2012). The object oriented classification approach avoids the so-called salt-and-pepper effect that commonly results when pixel-based remote sensing classification approaches are used. The landscape maps presented five classes: forest, built-up area, farmland, grassland, and water bodies.

### *Generating transition area matrix*

In this study, two pairs of land-cover images (1990–2000 and 2000–2010) were applied to calculate the transition area matrices of land-cover types during the two corresponding periods. Each matrix records the number of pixels that are expected to vary from a class to another class in a specified period in the future. This part of the model according to the trends observed in the past, is used to estimate the replacement rate of one class by another class. These matrices are obtained using the Markov Chain model with a proportional error of 0.1. The transition area matrices for the year 2010 were created by overlaying the 1990 and 2000 classifications and delineating the change between the two time periods on a class-by-class basis. This information is used as the input of the Markov model to assist in determining the possibility of conversion of any pixels of a land-cover class (e.g., forest) to other land-cover classes (e.g., field) and vice versa.

### Generating transition potential maps

Preparing suitability maps for land-cover classes is difficult in terms of data and information availability. Incorporating all types of factors or constraints that exist within the study area seems impossible. In this paper, transition potential maps of land-cover types were extracted by using GIS algorithms, multi-criteria evaluation (MCE), and fuzzy membership functions. Firstly, two drivers including neighborhood interaction (Euclidean distance to the same type cell) and conditional probability image were selected to compute transition potential maps of forest, grassland and farmland areas. As a rule of thumb, the pixel closer to an existing land-cover class has the higher possibility to change into that particular class. Since this rule cannot be applied to all situations (Ahmed and Ahmed 2012), the conditional probability images are used for each category to reduce uncertainty in the transition potential maps. The conditional probability images show, to what extent, each pixel in the next time period will likely belong to the designated category; and since this probability is conditional on their current state, they are referred to as conditional probability images. Therefore, these images are a visual presentation of the transition probability matrix (El-Hallaq and Habboub 2015). Restrictions for forest, grassland, and farmland were the built-up areas and water bodies. Finally, four typical biophysical and proximate drivers including slope, distance from nearest road, neighborhood interaction, and distances from water bodies were selected to compute transition potential map of built-up areas (Table 1). Also, water bodies considered as restriction area for built-up lands. Studies have shown that these ancillary data are closely related to the probability of urban changes (He et al. 2013; Yang et al. 2014).

Since Markov chain does not locate the occurrence of land-cover transitions, GIS algorithms, multi-criteria evaluation (MCE), and fuzzy membership functions were

applied to determine the suitability and locations of transitioning cells. The fuzzy sets create a standardized measure and avoid the selection of a priori unknown Boolean restrictions or cut-off values (Eastman 2006). Hence, the fuzzy membership functions (e.g., sigmoidal monotonic decrease function) were used to rescale driver maps into the range 0–255, where 0 represents unsuitable sites and 255 represents the most suitable sites. Also, analytic hierarchy process (AHP), as part of MCE, was applied to determine the weights of driving factors by means of pairwise assessments (Malczewski 1999). The AHP method allows weighting of land-cover transition potential on the basis of a set of potential maps (e.g., magnitude of slope), and incorporates growth constraints. The AHP affords a comprehensive and rational framework to solve the decision problem, characterizing and quantifying its elements, correlating the related elements towards overall goals, and evaluating alternative solutions. This GIS-based AHP is a strong tool because of its high ability to incorporate different types of heterogeneous variables and its simplicity to gain the weights of suitable variables (Hafeez et al. 2002; Ying et al. 2007). This model has a unique advantage when the quantification and comparison of important variables is difficult, or where the establishment of communications between working team members becomes problematic by their various specializations, terminologies, or perspectives. Because the areas of water is small, transition potentials to water is not computed. A set of transition potential maps are displayed in Fig. 2.

### Model evaluation

The evaluation of a model is an important step in the modeling process although there is no consensus on the criteria to assess the performance of landscape change models (Pontius 2000). The model is evaluated to detect whether the projected land-cover map is giving any abrupt

**Table 1** Extracted weights based on AHP and fuzzy standardization for built-up areas

Factors	Functions	Control points	Weights
Distance from roads	J-shaped	0–50 m highest suitability 50–1500 m decreasing suitability >1500 m no suitability	0.28
Distance from water bodies	Linear	0–100 m no suitability 100–7500 m increasing suitability >7500 m highest suitability	0.15
Distance from built-up areas	Linear	0–100 m highest suitability 100–5000 km decreasing suitability >5000 km no suitability	0.38
Slope	Sigmoid	0 % highest suitability 0–15 % decreasing suitability >15 % no suitability	0.19



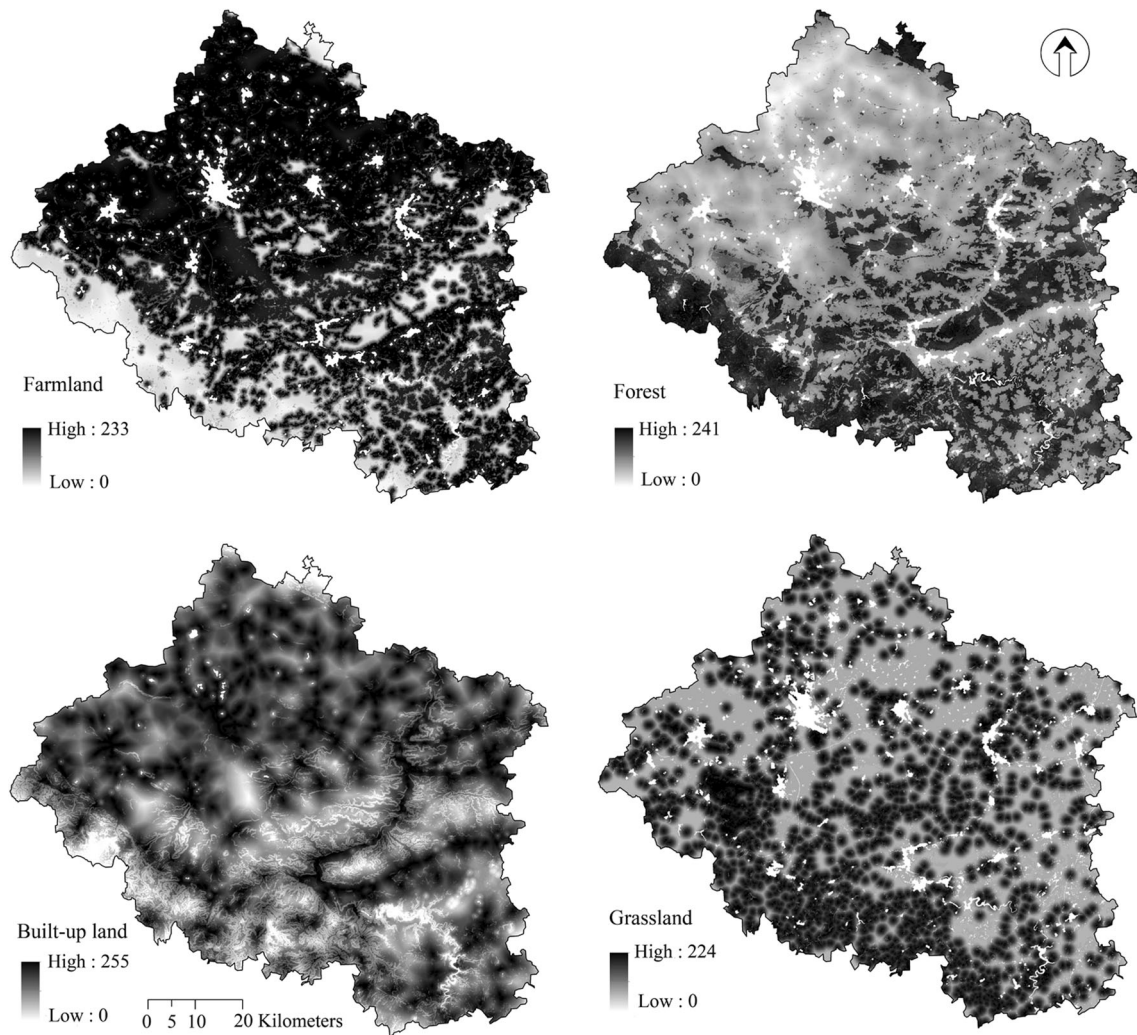


**Fig. 2** Transition potential maps of land-cover type in 2010

result or not. To validate the operation of a model the simulated map compares with the real conditions. This method has been favored in other studies such as by Araya and Cabral (2010) who used it to verify the accuracy of a model predicting land-cover change. The comparisons between the actual map of 2010, which was obtained through remote sensing techniques, and the projected map of year 2010, which observed using changes between 1990 and 2000 images, has been performed using Kappa variation statistics. Kappa is a very popular and well recognized map comparison index (Long and Giri 2011). The kappa statistics assess the model accuracy in terms of the quantity of cells properly classified along with the location of the cells.

Three kappa statistics are introduced here: the traditional kappa ( $K_{standard}$ ) which is a measure of the simulated layers' ability to attain perfect classification, a modified general statistic over  $K_{standard}$  ( $K_{no}$ ) which shows the

proportion of pixels classified correctly relative to the expected proportion classified correctly with no ability to specify quantity or location, and  $K_{location}$  index that is able to distinguish locational accuracy of pixels in the simulation. Its range is from 0 (random location) to 1 (perfect location specification) (Pontius 2000).

#### CA–Markov model

CA–Markov modeling is a hybrid modeling technique that binds the strengths of a spatially explicit, deterministic modeling framework with a stochastically based temporal framework. This model is a combination of Markov chain and CA models which has become a robust method in terms of dynamic spatial phenomenon's simulation and future land-cover change prediction in time and space based on their current state and on ancillary information which may drive future transitions among land-cover

classes. These results can in turn be used for theoretical constructions and for scenario-based projections by recalibrating the ancillary data. Markov Chain is a strong model for predicting land change demand when changes and processes in the land-cover are ambiguous to explain. This model is one in which the future state of environment can be analyzed solely according to the previous state. Markov chain model is a stochastic process model that describes how likely one state is to change to another state and use this as the basis to project future changes. This is possible through the development of a transition probability matrix of land-cover change from time to time, which represents that the nature of the change can still be used to predict the next period. In this model, the transition probability can be seen for each phenomenon, but no information is supplied on the spatial distribution of these phenomena. Thus, the CA is used to characterize the spatial characters. CA model is comprised of a regular lattice framework where any cell in the lattice is in one of a defined number of states. These states either remain in their current state or change at every iteration or time step into a different state (O'Sullivan and Unwin 2003). The changes are initiated by a set of deterministic rules that are defined prior to the execution of this process. There are four parameters needed to run CA: (1) a cellular (or grid) space, (2) a neighborhood definition, (3) a set number of states, and (4) a set of transition rules. The strength of CA is that it can robustly simulate processes that play out across time and space in human and in natural systems. As such they offer a useful framework for exploring system interactions (White and Engelen 1994). Hence, CA manages spatial dynamics via local transition rules, while Markov processes depict temporal dynamics of land-cover classes based on transition probabilities (see Eastman 2006; for more information).

To generate future land-cover maps, the suitability images are coupled with base land-cover and the transition matrices in a process called multi-object land allocation. This process compares all pixels and their suitability for each land-cover class. Each pixel has the potential to be populated by each land-cover class during the simulation (except by restricted and unchangeable area). The class which has the highest suitability at that pixel will be the class that is chosen given the prior spatial constraints of the CA and the temporal step to be classified for the stated time period. The process executes for each land-cover class and runs through the process several times at each time period. By subtracting the least likely pixels to be included in each land-cover class, the process continues until the correct number of pixels has been identified for the land-cover class under investigation. Because this process has random elements, an iterative process was used to create the potential land-cover class for each period. In order to gauge which areas are most likely to be another area, several

iterations of this process were run and then combined into a frequency image. This image is the overlay of all the iterations for a given land-cover class at a given time period and shows the proportion of times each cell was classified as a given land-cover class.

## Results

### Land-cover classification and accuracy assessment

An object-oriented image analysis was applied to produce a multi-temporal land-cover geographic database for the 3 years under study. In order to use the derived maps for further change analysis, the classification accuracy were estimated. To assess the accuracy of classified images, we gathered ground truth data (training and validation data) based on Quickbird images available in Google Earth (<http://earth.google.com>). For whole of study area, a sample of ground truth points randomly collected within the area covered by high resolution Quickbird images, overlaid selected points on the Quickbird images in Google Earth, and then grouped these points to appropriate classes based on visual interpretation. A point was considered as an especial class if land-cover patches covered at least one Landsat pixel ( $30 \times 30$  m). Based on visual interpretation of the Landsat images, the training sites were carefully determined and restricted to homogeneous regions where class membership was stable between 1990 and 2010. We optimized the training sample dataset until we achieved maximum stable accuracy. This optimizing task was carried out by removing training samples that may have been sources of error or collecting new samples to obviously misclassified categories. Finally, we used a sample of 1374 points were mapped from Quickbird images. We split all ground truth points into training (85 %) and evaluation (15 %) data. Overall accuracies for the extract land-cover maps of 1990, 2000 and 2010 were, respectively, 89.75, 92.36 and 93.54 %, thus indicating the suitability of the classified remote sensing images for effective and reliable land-cover change analysis and modeling. We finally used 100 % of the ground truth data to produce land-cover maps of the whole study area. Figure 3 illustrates the produced land-cover maps.

### Analysis of landscape metrics

Analysis of land-cover area changes in Table 2 indicate that from 1990 to 2010, built-up areas increased from 2.8 to 5.5 %. For the period between 1990 and 2000, around 7000 ha have been changed to built-up lands, and 10,980 ha within the period 2000–2010. The built-up land was continuously increased, and the farmland, grassland

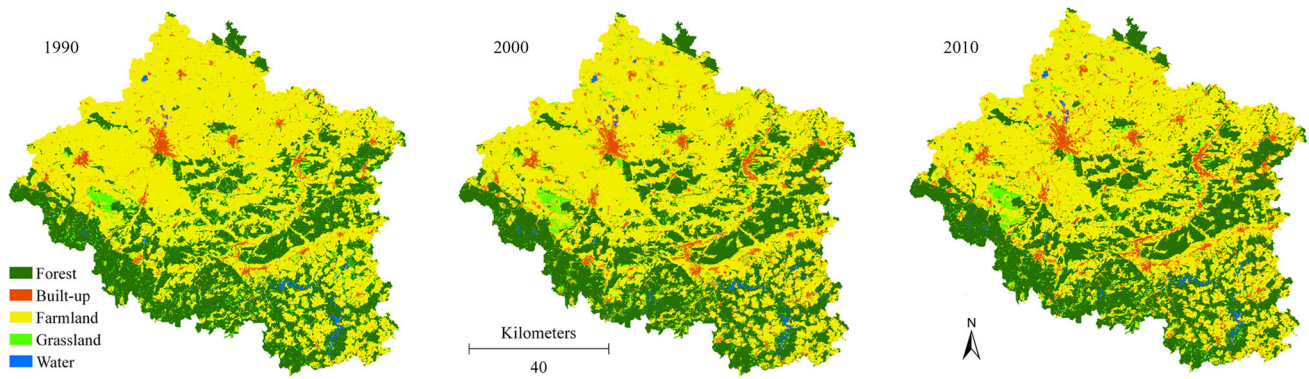


**Fig. 3** Time series of land-cover maps for 1990–2010

**Table 2** Distribution of land-cover classes (in hectare) and percentage of changes for 1990–2010

	Year			Change in land-cover structure		
	1990	2000	2010	$\Delta$ %1990–2000	$\Delta$ %2000–2010	$\Delta$ %1990–2010
Forest	223,400	222,810	222,550	−0.26	−0.12	−0.38
Water	4460	4530	4550	1.57	0.44	2.02
Grassland	33,750	31,390	27,750	−6.99	−11.60	−17.78
Farmland	408,490	404,370	397,270	−1.01	−1.76	−2.75
Built-up land	19,840	26,840	37,820	35.28	40.91	90.63

and forest were continuously decreased. Grasslands decreased significantly from 337.5 ha (4.89 %) to 277.5 ha (4.02 %) during 1990–2010. During this period, forest area decreased from 223400 ha (32.38 %) to 222550 ha (32.26 %). Also, farmlands reduced by 2.75 % from 1990 to 2010. Overall, farmlands lost around 11220 ha in this time period. The area of water increased a little.

**Analysis of transition matrix**

Transition matrices generated by the Markov model provide information about the amount of change and likelihood of change occurring before the final CA–Markov model was produced. In this section, transition potentials were computed based on land-cover conditions during the periods 1990–2000 and 2000–2010 to show how each land-cover was projected to change. Transition area matrices were compared to the total known areas of land derived from the classifications. The transition probability matrices give the likelihood of transition between phenomena over time (Table 3). The data on the diameter of transition probability illustrate the probability of a phenomenon remaining the same, while the off-diagonal data depict the change potential from one phenomenon to another (Guan et al., 2011). For example, the Markov transition probability matrix shows that the probability of future changes of grassland to forest from 1990 to 2000 is 13.3 %. This probability of change decreased reasonably to 10.9 % in

2010. Table 3 illustrates that for both periods, farmland and grassland possessed the highest likelihood of transforming into built-up areas. Overall, one trend is that over both periods the probability of remaining in the same class increased. Water bodies experienced the biggest increase between the first and second projections. After 10 years, there is an 89.7 % chance a current water pixel will still be water however after twenty years that value increases to 97.1 %.

**Land-cover modeling and validation**

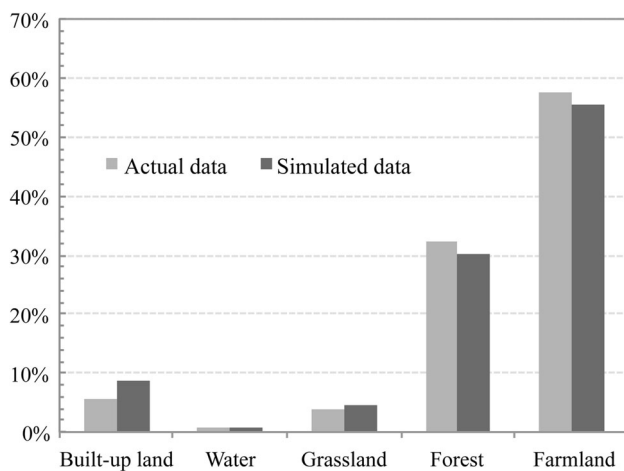
Evaluation of model was performed by comparing the simulated map of 2010 with the real land-cover map of 2010 based on Kappa variations. The change trajectories between the observed and simulated land-cover classes for the year 2010 are shown in Fig. 4, in which five land-cover classes have relative errors lower than 5 %.

Models with accuracies in excess of 80 % are typically considered very strong predictive tools (Araya and Cabral 2010). The  $K_{standard}$  value was 87.6 %, which verifies the accuracy of this model. Pontius (2000) states that the  $K_{no}$  value is a better alternative than  $K_{standard}$  for assessing the overall accuracy of the model. The model performed very well in its overall ability to predict land-cover map of 2010 ( $K_{no} = 91.5 \%$ ), and the  $K_{location}$  value of 92.2 % indicates that the model provides a reasonable representation of location. Also, visual interpretation of the results (Fig. 5)



**Table 3** Transition probability matrix of land-cover types for the periods 1990–2000 and 2000–2010

Land-cover type	Forest	Built-up land	Farmland	Grassland	Water bodies
1990–2000					
Forest	0.9346	0.0087	0.0193	0.0349	0.0025
Built-up land	0.0102	0.9276	0.0428	0.0118	0.0076
Farmland	0.0046	0.0602	0.8686	0.0657	0.0008
Grassland	0.1332	0.0417	0.061	0.7627	0.0014
Water bodies	0.078	0.0185	0.0056	0.0001	0.8978
2000–2010					
Forest	0.9247	0.003	0.0404	0.0295	0.0024
Built-up land	0.0094	0.9643	0.0076	0.0122	0.0065
Farmland	0.0107	0.0341	0.9076	0.0475	0.0001
Grassland	0.1095	0.0424	0.0496	0.7982	0.0003
Water bodies	0.0135	0.0083	0.005	0.0017	0.9715

**Fig. 4** Actual and simulated land-cover classes for the year 2010

shows that there is an evident similarity between the real and simulated maps for the year 2010. Therefore, based on the Kappa values obtained, the CA–Markov model can be used to simulate future land-cover conditions.

In this research, patterns and tendency of land-cover changes were modeled according to the preceding land-cover states. Although probabilities of land-cover transition are determined on a per category basis, the spatial distribution of phenomena in this analysis is lacking. Hence, the Markov model needs to be integrated with the CA model in order to add spatial characters to the model and to overcome this inherent limitation. In effect, by defining the land-cover map of 2010, the transition suitability maps derived from MCE analysis and Markov model (conditional probability images), transition area matrices of the land-cover maps of 2000–2010, a contiguity filter selection ( $5 \times 5$  Moore neighborhood kernel) to define neighborhood interactions, and one iteration per year were

employed to predict the future changes in 2020–2050. The contiguity filter down-weights the suitability of pixels that are far from existing areas of each land-cover class. The role of this filter is to ensure that the best choices for land-cover transformation are limited to cells that are both inherently suitable and in close proximity to existing areas of that land-cover class; this gives preference to contiguous suitable areas. In each iteration, pixels with the highest transition probability to transfer from one category to another category turn into a new category; while pixels with lower probabilities remain unchanged. If 10 iterations are selected for the model, the model allocates one tenth of all cells which are expected to be transferred to another category during each repetition (Eastman 2006). The multi-objective land allocation (MOLA) procedure was used to resolve the land allocation conflicts. All land-cover classes act as claimant phenomena and contend for land within the host class (Eastman 2006).

The outcome of this process was a rendering of a potential land-cover distribution at the specified time of 40 years into the future at four steps of 10 years. Ten years for each time step was chosen as it corresponded to the time step by which the transition matrix was constructed (between the years 2000–2010). Firstly, 2010 year is set as starting year; transition area matrix of 2000–2010 periods is used to simulate 2020 year land-cover change; then, 2020 year is set as starting year; transition area matrix of 2000–2010 periods is used to simulate 2030 year land-cover change; thirdly, 2030 year is set as starting year; transition area matrix of 2000–2010 periods is used to simulate 2040 year land-cover change; finally, 2040 year is set as starting year; transition area matrix of 2000–2010 periods is used to simulate 2050 year land-cover change. The forecasted land-cover maps for 2020 to 2050 are displayed in Fig. 6.



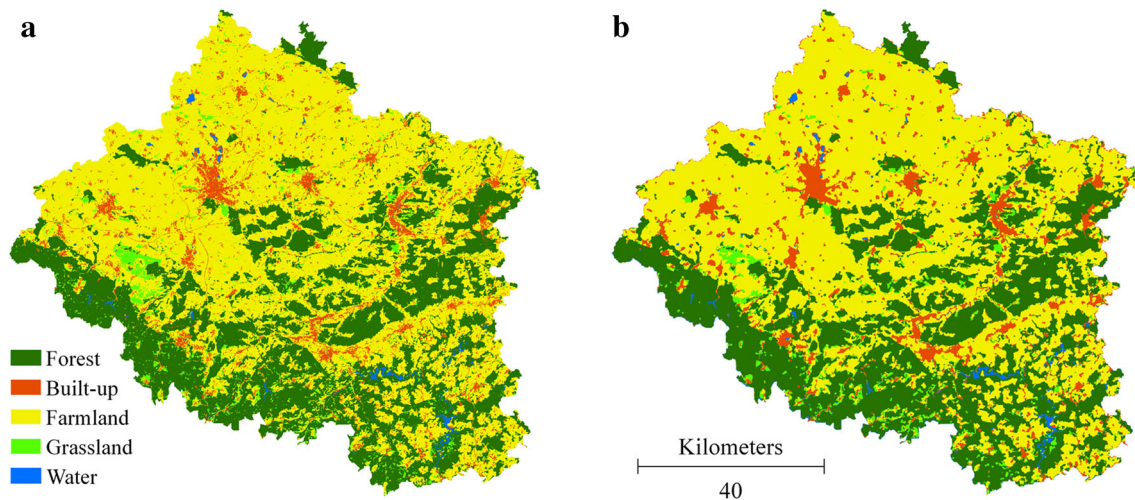


**Fig. 5** **a** Actual map and **b** simulated map of land-cover type in 2010

### Analysis of simulation results

Our results indicate that 5.5 % of the entire study area has been occupied as a built-up area in 2010, which will increase to 10.5 % by 2050, while for the other land-cover types (except water class), descending rate will observe by 2050 (Table 4). For example, grassland area was seen to decline from 27750 ha (4 %) to 15,730 ha (29.3 %) during 2010–2050. Also, for the other two land-cover classes, similar trends were observed, i.e. from 222,550 ha (32.3 %) to 217410 ha (32.5 %) and 397270 ha (57.6 %) to 379510 ha (55 %) for forest and farmland, respectively.

### Discussion and conclusion

The study reported here investigated land-cover changes over three time periods, 1990–2000, 2000–2010 and 2010–2050 using multi-temporal remote sensing data and GIS. Our results indicate that built-up areas dramatically increased by 90.6 % from 1990 to 2010. Overall, 17,980 ha have been changed to built-up areas in this time period. This suggests that the development of urban and rural areas in the past two decades has been a high pace. Araya and Cabral (2010) reported such a high rate of growth in their study area between the years 1990 to 2006. It highlights the fact that an increase in built-up area could be interpreted as a decrease in natural lands (Nature land = Total land area – (Farmland area + Built-up area); Lambin and Meyfroidt 2011). Table 2 shows that natural areas decreased from 254,852 ha in 1990 to 237,950 ha in 2010. For example forest lost 850 ha of its cover from 1990 to 2010. Degradation and loss of natural and semi-natural lands has become a profound concern which almost has affected the

entire Western and Central Europe (CBD 2010; GBO3 2010; Poschlod et al. 2005; Riecken et al. 2008).

The results of this study revealed that between the years 1990–2010, grasslands have lost a greater percentage of their area compared with forest lands. Table 2 shows that grasslands have lost 17.7 % of their land, while forests have lost just 0.38 percent in the same period. These results confirmed the high vulnerability of grasslands in European regions. The grasslands are decreasing in our study area, while previous studies warned that grassland deterioration could have a significant impact on ecosystem services (i.e. the carbon cycle, regional economy and climate) (Angell and McClaran 2001; Le Houérou 1996; Wen et al. 2013). Despite the fact that grasslands are the habitat for more than 50 % of vascular plant species in Central Europe (Lind et al. 2009), the European Topic Centre for Biological Diversity (ETC-BD) reports that grasslands are among the endangered habitats in the European regions and only 20 % of them are in a favorable conditions (EU-COM 2009; Siehoff et al. 2011).

The U.S. office of Military Government (Settel 1946) reported that after the Second World War, timber exports from Germany were particularly heavy, and forest area dramatically decreased consequently. But with change of national and regional policies the rate of deforestation started to decline (FAO 2011). The effect of this policy change is also visible in the results of this study, so that deforestation in the second decade (2000–2010) was almost half (0.44) of the first decade (2000–1990), while a downward trend has accelerated in grasslands so that in the second decade, this area declined approximately 1.67 times more than the first decade.

Seen from Fig. 7, area change results show that built-up patches will increase in area by the year 2050. The built-up

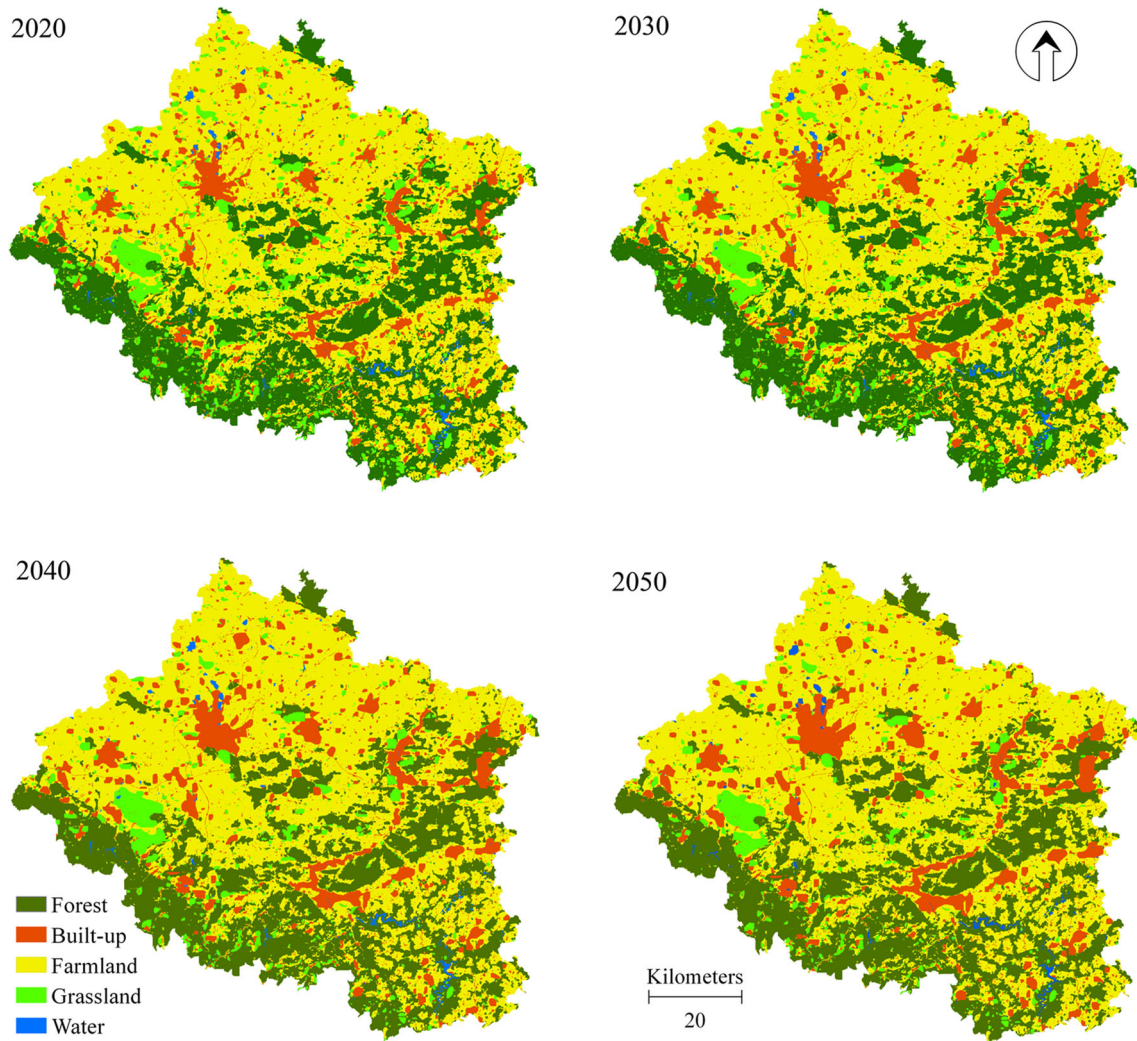


**Fig. 6** Simulated map of land-cover type from 2020 to 2050

**Table 4** Absolute quantities for land-cover classes (in hectare) for 2010–2050

	Built-up land	Forest	Water	Farmland	Grassland
2010	37,820	222,550	4552	397,270	27,750
2020	43,740	220,870	4630	394,710	25,990
2030	52,690	219,510	4680	388,940	24,120
2040	64,120	218,660	4730	382,150	20,280
2050	72,480	217,410	4810	379,510	15,730

areas are predicted to gain about 34,660 ha. While grasslands and forest areas would lose 12,020 and 5140 ha, respectively, in the same period. Seen from Fig. 6, spatial distribution results indicate that all land-cover classes would exhibit the concentrated spatial distribution patterns; urban built-up land would expand to suburban, because farmlands in the suburban areas would rapidly convert into built-up land.

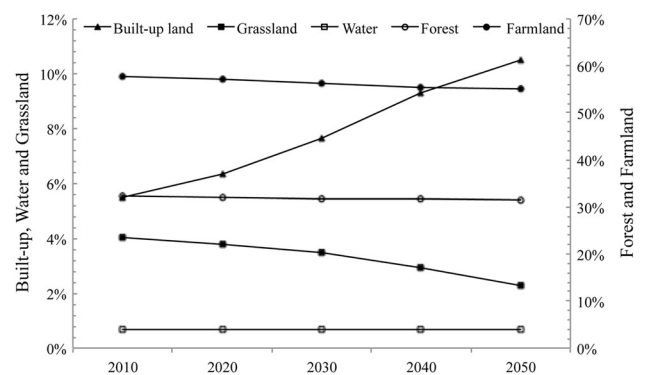


**Fig. 7** Area change of land-cover classes from 2010 to 2050

In total, results from CA–Markov models indicated a decrease in natural areas. The natural areas are expected to cover 31.5 % of our study area in year 2050, which means a 4.7 % decrease in comparison with its current

distribution. These results clearly showed the high degree of habitat loss and landscape fragmentation in study area which can break habitat connectivity and create a landscape mosaic of suitable, less suitable, and unsuitable habitat patches for species (Wiens et al. 2009). Due to the occurrences of less suitable habitats for establishment of species, the competition between species might increase. It is expected that competition among species significantly reduce their migration speed (Meier et al. 2012; Urban et al. 2012). Increasing competition and declining emigration, can lead to disappearing endangered species. Previous studies (Kinezaki et al. 2010; Meier et al. 2012) indicated that landscape changes will have a strong role in reducing the distribution areas of species in the coming decades, especially at a local scale (Engler et al. 2011; Pearson and Dawson 2003) like our study area.

Although the model used in this study has so well performed the simulation, there are a number of uncertainties in the projections of land-cover classes in the future, which are described as follows: First, it is important to note that some differences are evident between the observed and simulated land-cover maps of 2010. Accuracy of simulated land-cover changes will undoubtedly undergo image classification results (Araya and Cabral 2010). Although, object-based SVM is a very efficient classification method in handling complex class distributions (Huang et al. 2002; Pal and Mather 2005), but the classified images are somewhat erroneous. This misclassification can be considered as an uncertainty source in such studies.

Second, inadequate suitability maps for modeling the land-cover classes and the shape of the contiguity filter used in this study have been another source of uncertainty discussed in various studies (Araya and Cabral 2010; Sun et al. 2007). The suitability maps used in this study have a great influence on the land-cover simulations. This is because they are used as rules during the modeling process. Different suitability maps will lead to different rules that in turn may produce utterly different results. Further research is required to investigate the sensitivity of the predictions to the suitability maps.

Third, although this study confirmed that the procedure used in the analysis of the Markov chain is an effective method to calculate the transition probabilities of land-cover classes; these procedures assumed that transition probabilities do not change over time. In other words, the land-cover changes in the future in this model form up on the basis of land-cover patterns that have been identified in the past. This issue causes uncertainty in the simulation of land-cover changes because the model is not able to assess the new processes occurring on land-cover structures. For example our results show that from 1990 to 2010, the transition probabilities from various lands to built-up areas were extremely high and future land changes simulated

based on these transition probabilities. But the evidence suggests that the reality will be something else. After the fall of the Berlin Wall in 1990, the need for modernization and spatial expansion in eastern regions (Former East Germany) was absolutely essential (Braun et al. 2012). As a result, a new framework for planning the urban development, termed “Critical Reconstruction”, was implemented in these areas (Neill and Schwedler 2001; Tölle 2010). The implementation of this policy caused open and empty areas within cities and many lands (i.e. agricultural lands) in the countryside to be converted quickly into industrial and urban areas after the year 1990 (Loeb 2006). Therefore, transition probability from other lands to built-up areas was extremely high in eastern regions (such as our study area) during these years. But, at present, the majority of these changes are over and it predicts that urban development (transition probability to built-up area) would significantly reduce in the coming years.

Finally, predicting future landscape changes would be full of uncertainty due to unpredictable events (such as fires and floods), effects of climate change (Vittoz et al. 2009), possible changes in managerial attitudes, and potential uncertainty which coming from simulator models.

Our analysis demonstrates that the integration of GIS, remote sensing, and land change modeling offers an enhanced understanding of the futures and trends that landscape will face. Facing to declining problems of natural lands, the simulated future land-cover maps can serve as an early warning system for understanding the future effects of land-cover changes. In sum, these notable relevant findings can also be considered as a strategic guide to land-cover planning, and help local authorities (policy makers, urban planning, natural resources managers and land-cover management organizations) better understand a complex land-cover system and develop the improved land-cover management that can better balance urban expansion and ecological environment conservation. To determine whether the patterns of projected landscape change are specific to our study area, this technique should be empirically repeated and needs more comparative studies.

**Acknowledgments** The authors would like to thank the Thüringer Landesanstalt für Umwelt und Geologie, Jena, Germany for providing digital data, and also the United States Geological Survey (USGS) and European Space Agency (ESA) for preparing free archive of Landsat Earth-observing satellites images.

## References

- Ahmed B, Ahmed R (2012) Modeling Urban Land Cover Growth Dynamics Using Multi-Temporal Satellite Images: a Case Study of Dhaka, Bangladesh. *ISPRS Int J Geo-Inf* 1:3
- Angell DL, McClaran MP (2001) Long-term influences of livestock management and a non-native grass on grass dynamics in the



- Desert Grassland. *J Arid Environ* 49:507–520. doi:[10.1006/jare.2001.0811](https://doi.org/10.1006/jare.2001.0811)
- Araya YH, Cabral P (2010) Analysis and modeling of urban land cover change in Setubal and sesimbra. *Port Remote Sens* 2:1549–1563
- Bagan H, Yamagata Y (2012) Landsat analysis of urban growth: how Tokyo became the world's largest megacity during the last 40years. *Remote Sens Environ* 127:210–222. doi:[10.1016/j.rse.2012.09.011](https://doi.org/10.1016/j.rse.2012.09.011)
- Balmford A, Moore JL, Brooks T, Burgess N, Hansen LA, Williams P, Rahbek C (2001) Conservation conflicts across Africa. *Science* 291:2616–2619. doi:[10.1126/science.291.5513.2616](https://doi.org/10.1126/science.291.5513.2616)
- Basse RM, Omrani H, Charif O, Gerber P, Bódis K (2014) Land use changes modelling using advanced methods: cellular automata and artificial neural networks, The spatial and explicit representation of land cover dynamics at the cross-border region scale. *Appl Geogr* 53:160–171. doi:[10.1016/j.apgeog.2014.06.016](https://doi.org/10.1016/j.apgeog.2014.06.016)
- Braun E, van den Berg PL, van der Meer J (2012) National policy responses to urban challenges in Europe. Ashgate Publishing Limited, Aldershot
- Castella J-C, Pheng Kam S, Dinh Quang D, Verburg PH, Thai Hoanh C (2007) Combining top-down and bottom-up modelling approaches of land use/cover change to support public policies: application to sustainable management of natural resources in northern. *Vietnam Land Use Policy* 24:531–545. doi:[10.1016/j.landusepol.2005.09.009](https://doi.org/10.1016/j.landusepol.2005.09.009)
- CBD (2010) Fourth national report under the convention on biological diversity (CBD)—Germany. <http://www.cbd.int/reports/search/>
- Deng X, Huang J, Rozelle S, Uchida E (2008) Growth, population and industrialization, and urban land expansion of China. *J Urban Econ* 63:96–115. doi:[10.1016/j.jue.2006.12.006](https://doi.org/10.1016/j.jue.2006.12.006)
- Duro DC, Franklin SE, Dubé MG (2012) A comparison of pixel-based and object-based image analysis with selected machine learning algorithms for the classification of agricultural landscapes using SPOT-5 HRG imagery. *Remote Sens Environ* 118:259–272. doi:[10.1016/j.rse.2011.11.020](https://doi.org/10.1016/j.rse.2011.11.020)
- Eastman JR (2006) IDRISI andes. Clark University, Worcester
- El-Hallaq MA, Habboub MO (2015) using cellular automata–markov analysis and multi criteria evaluation for predicting the shape of the dead sea advances in remote sensing, Vol. 04 No. 01:13 doi:[10.4236/ars.2015.41008](https://doi.org/10.4236/ars.2015.41008)
- Engler R et al (2011) 21st century climate change threatens mountain flora unequally across Europe. *Glob Change Biol* 17:2330–2341. doi:[10.1111/j.1365-2486.2010.02393.x](https://doi.org/10.1111/j.1365-2486.2010.02393.x)
- EU-COM (2009) Composite report on the conservation status of habitat types and species as required under Article 17 of Habitats directive. Report from the Commission to the Council and the European Parliament, Brussels
- FAO (2011) State of the world's forests. Forestry Department, Rome
- Funkenberg T, Binh TT, Moder F, Dech S (2014) The Ha Tien plain—wetland monitoring using remote-sensing techniques. *Int J Remote Sens* 35:2893–2909. doi:[10.1080/01431161.2014.890306](https://doi.org/10.1080/01431161.2014.890306)
- GBO3 (2010) Secretariat of the convention on biological diversity. Global Biodiversity Outlook 3—Executive Summary, Montreal
- Guan D, Li H, Inohae T, Su W, Nagaie T, Hokao K (2011) Modeling urban land use change by the integration of cellular automaton and Markov model. *Ecol Model* 222:3761–3772. doi:[10.1016/j.ecolmodel.2011.09.009](https://doi.org/10.1016/j.ecolmodel.2011.09.009)
- Hafeez K, Zhang Y, Malak N (2002) Determining key capabilities of a firm using analytic hierarchy process. *Int J Prod Econ* 76:39–51. doi:[10.1016/S0925-5273\(01\)00141-4](https://doi.org/10.1016/S0925-5273(01)00141-4)
- He J, Liu Y, Yu Y, Tang W, Xiang W, Liu D (2013) A counterfactual scenario simulation approach for assessing the impact of farmland preservation policies on urban sprawl and food security in a major grain-producing area of China. *Appl Geogr* 37:127–138. doi:[10.1016/j.apgeog.2012.11.005](https://doi.org/10.1016/j.apgeog.2012.11.005)
- Houghton RA (1994) The Worldwide extent of land-use change: in the last few centuries, and particularly in the last several decades, effects of land-use change have become global. *Bioscience* 44:305–313. doi:[10.2307/1312380](https://doi.org/10.2307/1312380)
- Hu Z, Lo CP (2007) Modeling urban growth in Atlanta using logistic regression. *Comput Environ and Urban Syst* 31:667–688. doi:[10.1016/j.compenvurbsys.2006.11.001](https://doi.org/10.1016/j.compenvurbsys.2006.11.001)
- Huang C, Davis LS, Townshend JRG (2002) An assessment of support vector machines for land cover classification. *Int J Remote Sens* 23:725–749. doi:[10.1080/01431160110040323](https://doi.org/10.1080/01431160110040323)
- Jetz W, Wilcove DS, Dobson AP (2007) Projected impacts of climate and land-use change on the global diversity of birds. *PLoS Biol* 5:e157. doi:[10.1371/journal.pbio.0050157](https://doi.org/10.1371/journal.pbio.0050157)
- Kamusoko C, Aniya M, Adi B, Manjoro M (2009) Rural sustainability under threat in Zimbabwe - Simulation of future land use/cover changes in the Bindura district based on the Markov–cellular automata model. *Appl Geogr* 29:435–447. doi:[10.1016/j.apgeog.2008.10.002](https://doi.org/10.1016/j.apgeog.2008.10.002)
- Kinezaki N, Kawasaki K, Shigesada N (2010) The effect of the spatial configuration of habitat fragmentation on invasive spread. *Theor Popul Biol* 78:298–308. doi:[10.1016/j.tpb.2010.09.002](https://doi.org/10.1016/j.tpb.2010.09.002)
- Kuenzer C, Leinenkugel P, Vollmuth M, Dech S (2014) Comparing global land-cover products—implications for geoscience applications: an investigation for the trans-boundary Mekong Basin. *Int J Remote Sens* 35:2752–2779. doi:[10.1080/01431161.2014.890305](https://doi.org/10.1080/01431161.2014.890305)
- Lambin EF, Meyfroidt P (2011) Global land use change, economic globalization, and the looming land scarcity. *Proc Natl Acad Sci* 108:3465–3472. doi:[10.1073/pnas.1100480108](https://doi.org/10.1073/pnas.1100480108)
- Le Houérou HN (1996) Climate change, drought and desertification. *J Arid Environ* 34:133–185. doi:[10.1006/jare.1996.0099](https://doi.org/10.1006/jare.1996.0099)
- Leinenkugel P, Kuenzer C, Oppelt N, Dech S (2013) Characterisation of land surface phenology and land cover based on moderate resolution satellite data in cloud prone areas—a novel product for the Mekong Basin. *Remote Sens Environ* 136:180–198. doi:[10.1016/j.rse.2013.05.004](https://doi.org/10.1016/j.rse.2013.05.004)
- Lind B, Stein S, Kärcher A, Klein M (2009) Where have All the Flowers Gone? Grünland im Umbruch. German Federal Agency for Nature Conservation (BfN), Bonn
- Loeb C (2006) Planning reunification: the planning history of the fall of the Berlin Wall. *Plan Perspect* 21:67–87. doi:[10.1080/02665430500397329](https://doi.org/10.1080/02665430500397329)
- Long JB, Giri C (2011) Mapping the philippines' mangrove forests using landsat imagery. *Sensors* 11:2972
- Macedo MN, Coe MT, DeFries R, Uriarte M, Brando PM, Neill C, Walker WS (2013) Land-use-driven stream warming in south-eastern Amazonia. *Philos Trans R Soc Lond Series B Biol Sci* 368:20120153. doi:[10.1098/rstb.2012.0153](https://doi.org/10.1098/rstb.2012.0153)
- Malczewski J (1999) GIS and multicriteria decision analysis. Wiley, New York
- Meier ES, Lischke H, Schmatz DR, Zimmermann NE (2012) Climate, competition and connectivity affect future migration and ranges of European trees. *Glob Ecol Biogeogr* 21:164–178. doi:[10.1111/j.1466-8238.2011.00669.x](https://doi.org/10.1111/j.1466-8238.2011.00669.x)
- Mitsova D, Shuster W, Wang X (2011) A cellular automata model of land cover change to integrate urban growth with open space conservation. *Landscape Urban Plan* 99:141–153. doi:[10.1016/j.landurbplan.2010.10.001](https://doi.org/10.1016/j.landurbplan.2010.10.001)
- Neill WVJ, Schwedler HU (2001) Urban planning and cultural inclusion: lessons from Belfast and Berlin. Palgrave Macmillan
- O'Sullivan D, Unwin DJ (2003) Geographic information analysis. Wiley, Hoboken
- Pal M, Mather PM (2005) Support vector machines for classification in remote sensing. *Int J Remote Sens* 26:1007–1011. doi:[10.1080/01431160512331314083](https://doi.org/10.1080/01431160512331314083)
- Pearson RG, Dawson TP (2003) Predicting the impacts of climate change on the distribution of species: are bioclimate envelope



- models useful? *Glob Ecol Biogeogr* 12:361–371. doi:[10.1046/j.1466-822X.2003.00042.x](https://doi.org/10.1046/j.1466-822X.2003.00042.x)
- Pijanowski BC, Brown DG, Shellito BA, Manik GA (2002) Using neural networks and GIS to forecast land use changes: a land transformation model computers. *Environ Urban Syst* 26:553–575. doi:[10.1016/S0198-9715\(01\)00015-1](https://doi.org/10.1016/S0198-9715(01)00015-1)
- Pimm SL, Raven P (2000) Biodiversity. Extinction by numbers. *Nature* 403:843–845. doi:[10.1038/35002708](https://doi.org/10.1038/35002708)
- Poelmans L, Van Rompaey A (2010) Complexity and performance of urban expansion models. *Comput Environ Urban Syst* 34:17–27. doi:[10.1016/j.compenvurbsys.2009.06.001](https://doi.org/10.1016/j.compenvurbsys.2009.06.001)
- Pompe S, Hanspach J, Badeck F, Klotz S, Thuiller W, Kühn I (2008) Climate and land use change impacts on plant distributions in Germany. *Biol Lett* 4:564–567
- Pontius GR (2000) Quantification error versus location error in comparison of categorical maps. *Photogram Eng Remote Sens* 66:1011–1016
- Poschlod P, Bakker JP, Kahmen S (2005) Changing land use and its impact on biodiversity. *Basic Appl Ecol* 6:93–98. doi:[10.1016/j.baae.2004.12.001](https://doi.org/10.1016/j.baae.2004.12.001)
- Rai SC, Sharma E (1998) Comparative assessment of runoff characteristics under different land use patterns within a Himalayan watershed. *Hydrol Process* 12:2235–2248
- Ramankutty N, Foley JA (1998) Characterizing patterns of global land use: an analysis of global croplands data. *Global Biogeochem Cycles* 12:667–685. doi:[10.1029/98GB02512](https://doi.org/10.1029/98GB02512)
- Riecken U, Finck P, Raths U, Schröder E, Ssymank A (2008) Die Gefährdung der Biotoptypen in Deutschland Aktueller Stand nach Vorlage der 2 Fassung der Roten Liste Natursch Biol Vielf 60:189–194
- Sala OE et al (2000) Global biodiversity scenarios for the year 2100. *Science* 287:1770–1774
- Sang L, Zhang C, Yang J, Zhu D, Yun W (2011) Simulation of land use spatial pattern of towns and villages based on CA–Markov model. *Math Comput Model* 54:938–943. doi:[10.1016/j.mcm.2010.11.019](https://doi.org/10.1016/j.mcm.2010.11.019)
- Settel A (1946) A year of Potsdam: the German economy since the surrender. Lithographed by the Adjutant General, OMGUS
- Sidle RC, Ziegler AD, Negishi JN, Nik AR, Siew R, Turkelboom F (2006) Erosion processes in steep terrain—truths, myths, and uncertainties related to forest management in Southeast Asia. *For Ecol Manage* 224:199–225. doi:[10.1016/j.foreco.2005.12.019](https://doi.org/10.1016/j.foreco.2005.12.019)
- Siehoff S, Lennartz G, Heilburg IC, Roß-Nickoll M, Ratte HT, Preuss TG (2011) Process-based modeling of grassland dynamics built on ecological indicator values for land use. *Ecol Model* 222:3854–3868. doi:[10.1016/j.ecolmodel.2011.10.003](https://doi.org/10.1016/j.ecolmodel.2011.10.003)
- Subedi P, Subedi K, Thapa B (2013) Application of a hybrid cellular automaton–C Markov (CA–Markov) model in land-use change prediction: a case study of saddle creek drainage basin, Florida. *Appl Ecol Environ Sci* 1:126–132. doi:[10.12691/aees-1-6-5](https://doi.org/10.12691/aees-1-6-5)
- Sun H, Forsythe W, Waters N (2007) Modeling urban land use change and urban sprawl: calgary, Alberta, Canada. *Netw Spat Econ* 7:353–376. doi:[10.1007/s11067-007-9030-y](https://doi.org/10.1007/s11067-007-9030-y)
- Tölle A (2010) Urban identity policies in Berlin: from critical reconstruction to reconstructing the Wall. *Cities* 27:348–357. doi:[10.1016/j.cities.2010.04.005](https://doi.org/10.1016/j.cities.2010.04.005)
- Townshend J, Justice C, Li W, Gurney C, McManus J (1991) Global land cover classification by remote sensing: present capabilities and future possibilities. *Remote Sens Environ* 35:243–255. doi:[10.1016/0034-4257\(91\)90016-Y](https://doi.org/10.1016/0034-4257(91)90016-Y)
- Urban MC, Tewksbury JJ, Sheldon KS (2012) On a collision course: competition and dispersal differences create no-analogue communities and cause extinctions during climate change. *Proc R Soc Lond B Biol Sci* 279:2072–2080
- Vitousek PM (1994) Beyond global warming: ecology and global change. *Ecology* 75:1861–1876. doi:[10.2307/1941591](https://doi.org/10.2307/1941591)
- Vittoz P, Randin C, Dutoit A, Bonnet F, Hegg O (2009) Low impact of climate change on subalpine grasslands in the Swiss Northern Alps. *Global Change Biol* 15:209–220. doi:[10.1111/j.1365-2486.2008.01707.x](https://doi.org/10.1111/j.1365-2486.2008.01707.x)
- Wen L et al (2013) Effect of degradation intensity on grassland ecosystem services in the alpine region of Qinghai-Tibetan Plateau, China. *PLoS ONE* 8:e58432. doi:[10.1371/journal.pone.0058432](https://doi.org/10.1371/journal.pone.0058432)
- White R, Engelen G (1994) Cellular dynamics and GIS: modelling spatial complexity. *J Geogr Syst* 1:237–253
- Wiens JA, Stralberg D, Jongsomjit D, Howell CA, Snyder MA (2009) Niches, models, and climate change: assessing the assumptions and uncertainties. *Proc Natl Acad Sci USA* 106:19729–19736. doi:[10.1073/pnas.0901639106](https://doi.org/10.1073/pnas.0901639106)
- Yang X, Zheng X-Q, Lv L-N (2012) A spatiotemporal model of land use change based on ant colony optimization, Markov chain and cellular automata. *Ecol Model* 233:11–19. doi:[10.1016/j.ecolmodel.2012.03.011](https://doi.org/10.1016/j.ecolmodel.2012.03.011)
- Yang X, Zheng X-Q, Chen R (2014) A land use change model: integrating landscape pattern indexes and Markov-CA. *Ecol Model* 283:1–7. doi:[10.1016/j.ecolmodel.2014.03.011](https://doi.org/10.1016/j.ecolmodel.2014.03.011)
- Ying X, Zeng G-M, Chen G-Q, Tang L, Wang K-L, Huang D-Y (2007) Combining AHP with GIS in synthetic evaluation of eco-environment quality—a case study of Hunan Province. *China Ecol Model* 209:97–109. doi:[10.1016/j.ecolmodel.2007.06.007](https://doi.org/10.1016/j.ecolmodel.2007.06.007)